Metrological Characterization of a Calibrator for Static and Dynamic Validation of Distribution Network PMUs

G. Frigo, A. Derviškadić, M. Paolone

Swiss Federal Institute of Technology (EPFL)
Distributed Electrical Systems Laboratory (DESL)

Motivation of the Work

Active Distribution Networks (ADNs)

SOURCE: sine.ni.com

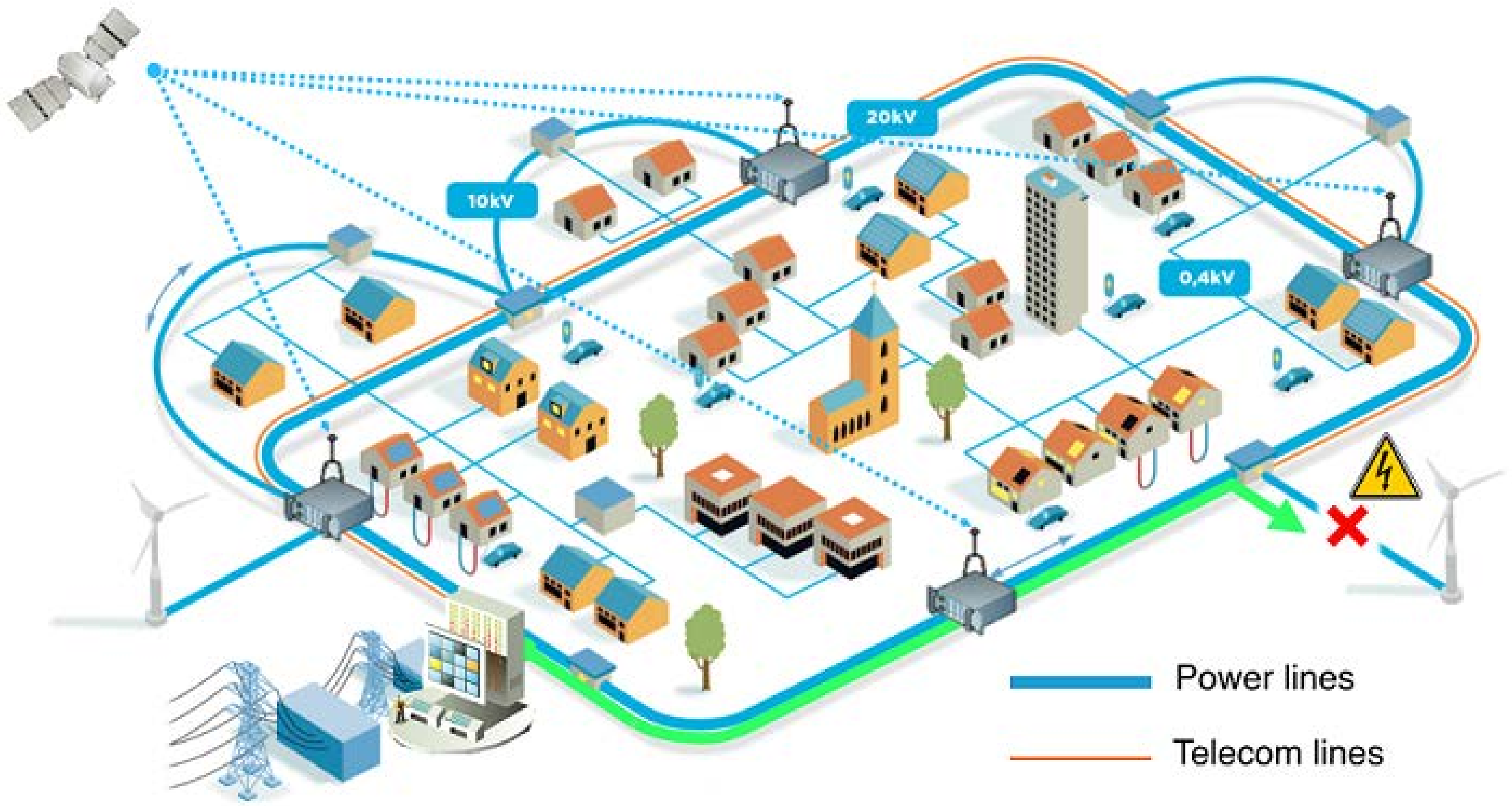

= Phasor Measurement Unit (PMU)

= Feeder Monitoring, Control Unit (PDC+RTSE+control+protection)

Motivation of the Work

Measurement challenges in ADNs

Compared to TNs, in ADNs waveform disturbances are more remarkable:

- **Harmonic distortion** beyond the IEEE Std. C37.118 specs.
  - Superposition of multiple harmonics (EN 50160).
  - Harmonics superposed to frequency fluctuations.
- **Higher measurement noise**, particularly in measured currents.
- R/X ratio close to 1, resulting in **limited phase difference**.
- **Reduced power flows**, limited to few MVA maximum.
- **Faster dynamics** w.r.t. renewables short-term volatility.

Solution: PMUs & Smart meters characterized by **enhanced accuracy (TVE$\leq 0.0x\%$ in static)**.

Motivation of the work

PMU accuracy requirements in ADNs

The “PMU calibrator” should provide a **reference accuracy at least 10X better than PMUs** under test .

Objective: to **develop** and **characterize** a **validation system** with **TVE$\leq 0.00x\%$** in static.

IEEE Std C37.118.1
TVE$\leq 1\%$

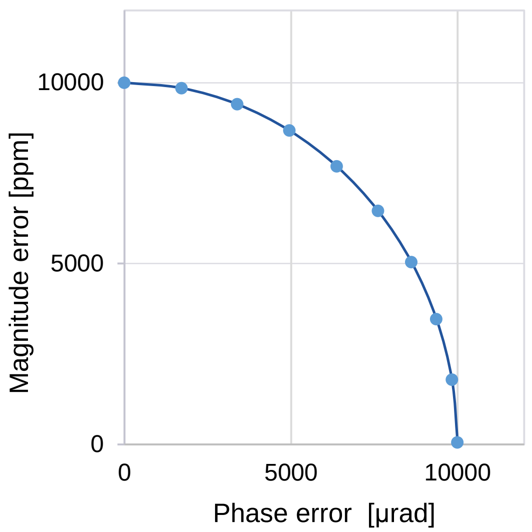

PMUs in ADNs
TVE$\leq 0.0x\%$

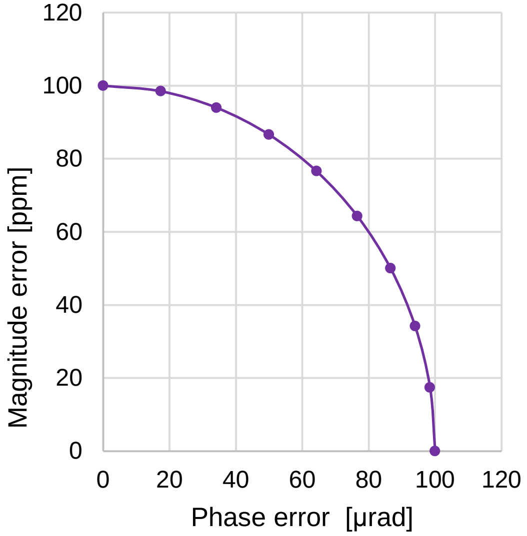

PMU calibrator
TVE$\leq 0.00x\%$

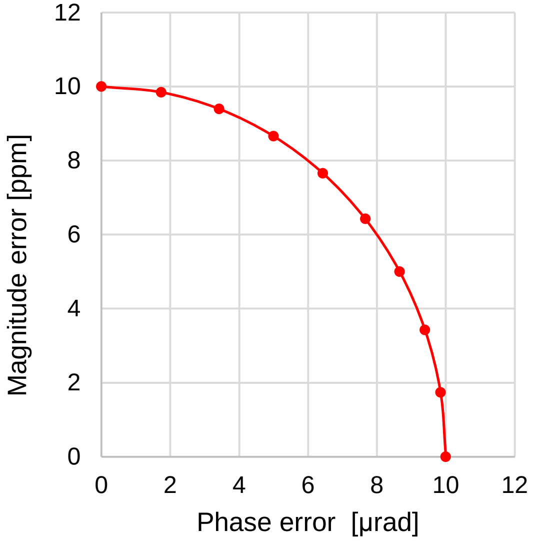

Presentation Outline

- Hardware Architecture
- Metrological Characterization
  - Reference value definition
  - Uncertainty contributions
- Phasor Analysis in Transient Events
- Conclusions

Presentation Outline

- Hardware Architecture
- Metrological Characterization
  - Reference value definition
  - Uncertainty contributions
- Phasor Analysis in Transient Events
- Conclusions

Hardware Architecture

Chassis

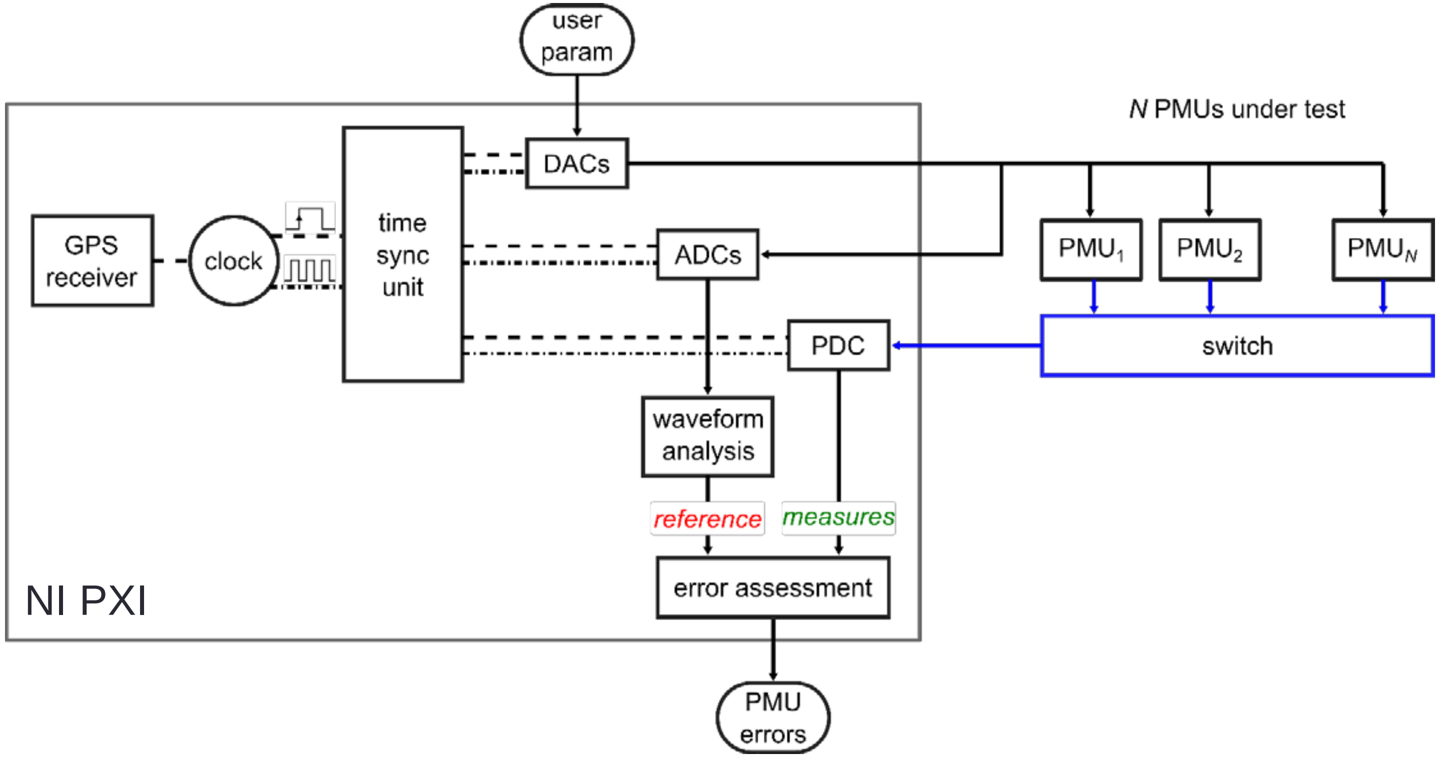

NI PXI 1042Q

- Compatible with external time-base reference sources ➔ disciplined by GPS receiver and Rb atomic clock;
- Integrated synchronization schemes via dedicated channels ➔ perfectly synchronous generation/acquisition;
- Embedded μ-controller (RAM 2 GB) ➔ data processing and analysis

Hardware Architecture

Time synchronization

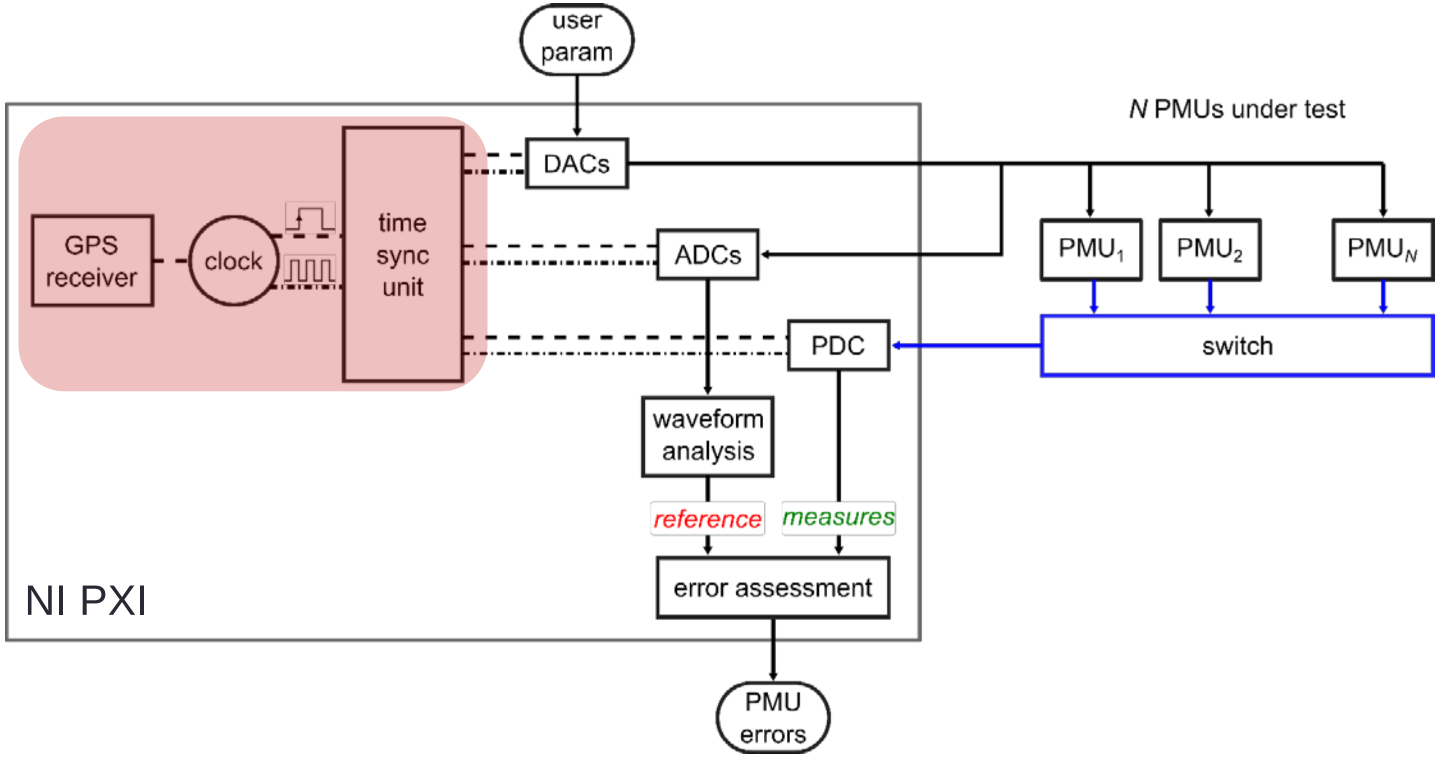

NI PXI 6682

- Disseminates the internal time-base within the other operational units;
- Rubidium atomic clock provides the 10 MHz and PPS (1 Hz) reference ➔ higher short-term stability;
- GPS receiver disciplines the atomic clock via PPS signal ➔ higher long-term stability

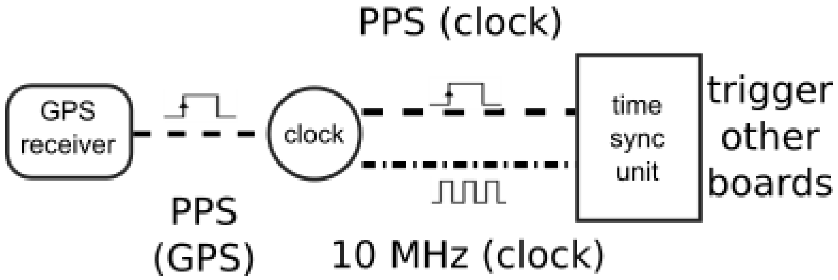

Hardware Architecture

Waveform generation

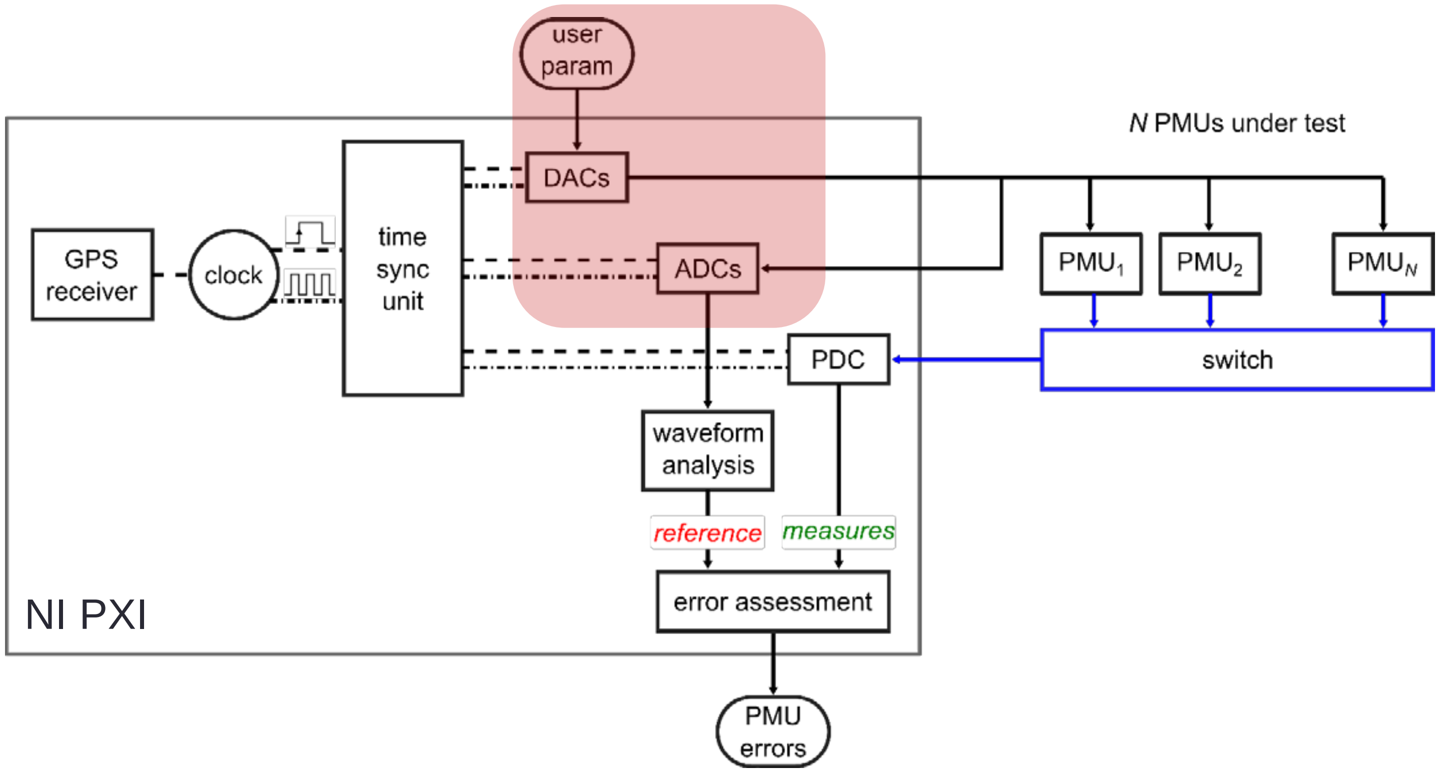

NI PXI 6289

- High-accuracy I/O data ➔ up to 100 kS/s (25 kS/s for 3 phase), at 16 bit;
- SNR = 93.5 dB, THD ≃ 10^{-5} %;
- Voltage range ±12 V ➔ compliant with MV/LV instrument transformer of IEC 61869;

Hardware Architecture

Phasor Data Concentrator (PDC)

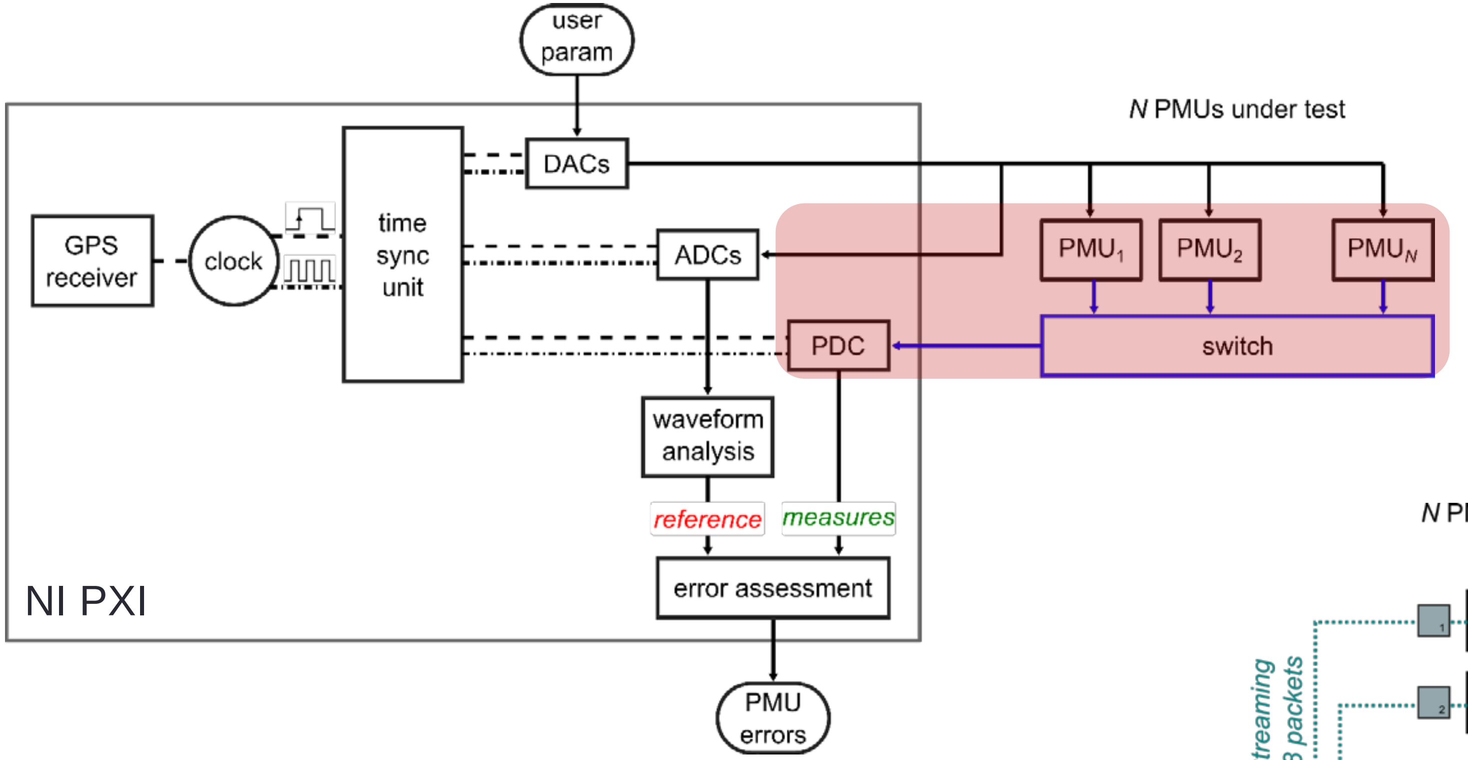

Optimized PDC

- Aggregation of measurement data from PMUs ➔ time-aligned based on timestamp;
- Single switch ➔ negligible latency introduced by network;

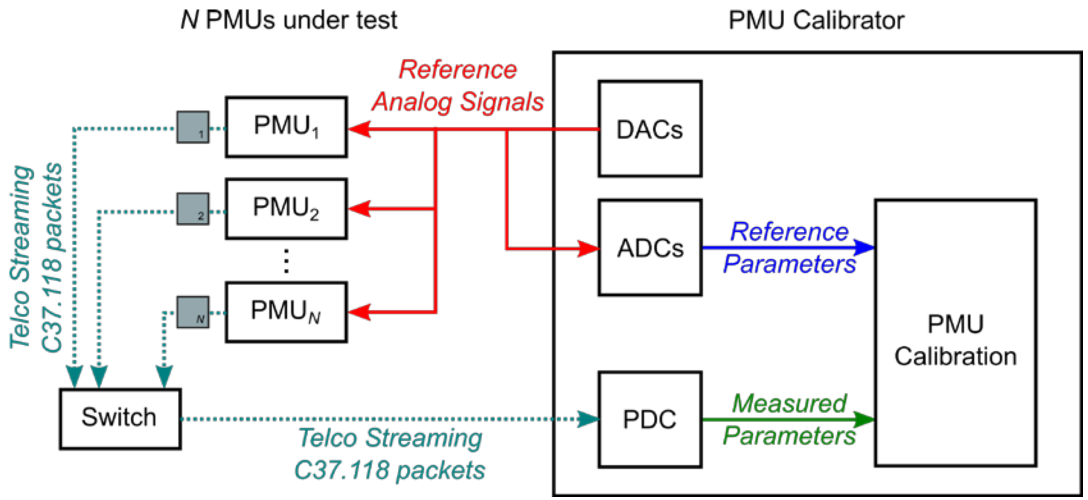

Hardware Architecture

Error assessment

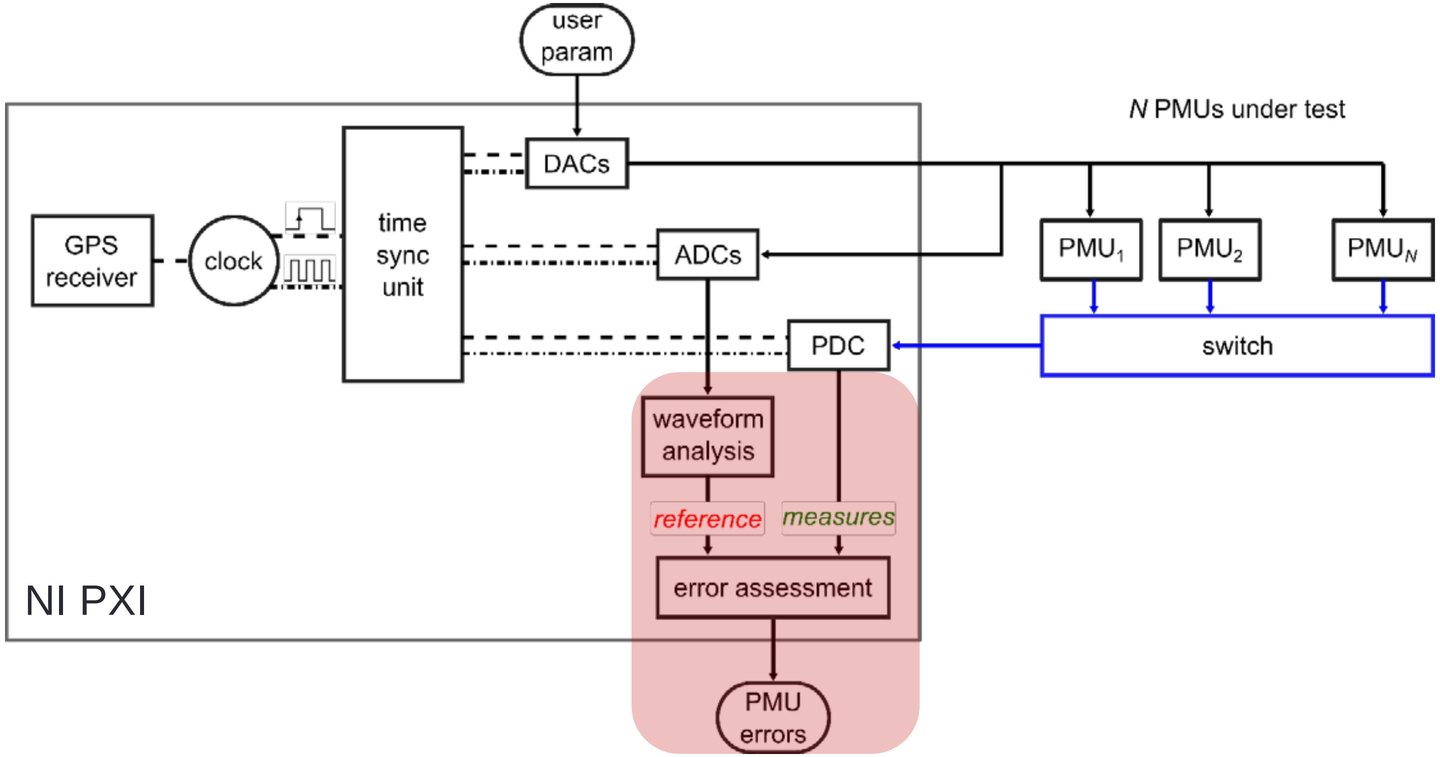

Error Assessment

- ADC waveform off-line processing ➔ reference values;
- Comparison with PMUs' measures ➔ TVE, FE and RFE;

Presentation Outline

- Hardware Architecture
- Metrological Characterization
  - Reference value definition
  - Uncertainty contributions
- Phasor Analysis in Transient Events
- Conclusions

Metrological Characterization

Reference values estimation

Signal model: generic time-variant noise-less power signal affected by disturbances:

$$x(t) = \mathbf{A}\left(1 + \varepsilon_A(t)\right) \cdot \cos\left(2\pi \mathbf{f} t + \boldsymbol{\varphi}_\mathbf{0} + \varepsilon_\varphi(t)\right) + \eta(t)$$

A, f, φ_0: amplitude, frequency and initial phase of **fundamental component**

ε_A, ε_φ: **amplitude and phase fluctuations** (e.g. modulations)

η: DC, **harmonic and inter-harmonic components** and any transient condition affecting the spectrum other than fundamental component transient

Metrological Characterization

Reference values estimation

Working HP: $\varepsilon_A(t), \varepsilon_\varphi(t)$ and $\eta(t)$ are **known a priori**

Reference values assessment via **non-linear least-squares (NL-LSQ) fit [1]**

$$\{\hat{A}, \hat{f}, \hat{\phi}_0\} = \text{argmin}_{\hat{\mathcal{P}}} \|x[n] - \hat{x}[n]\|_2$$

Input: $x(t)$ ➔ *waveform model*

$x[n]$ ➔ *acquired waveform*

$\mathcal{P}^* = \{A^*, f^*, \varphi_0^*\}$ ➔ *initial guess (user-defined parameters)*

Output: $\hat{\mathcal{P}} = \{\hat{A}, \hat{f}, \hat{\phi}_0\}$ ➔ *reference values*

$\hat{s} = \hat{A} \cdot \exp(1j\ 2\pi\hat{f}\ nT_s + \hat{\phi}_0)$ ➔ *reference synchrophasor*

$\hat{x}[n] = \hat{A} \cdot \cos(2\pi\hat{f}nT_s + \hat{\phi}_0)$ ➔ *recovered fundamental tone*

Metrological Characterization

NL-LSQ estimation accuracy

We characterized the NL-LSQ accuracy in all the **IEEE Std C37.118.1 static tests**, by simulating 3-phase voltage signals, with the same sampling rate, SNR and THD. The test signals have a duration of **5 s**.

NL-LSQ provides the reference synchrophasor related to **60-ms windows** with a **reporting rate of 50 fps**, in compliance with P-class PMUs but better performance can be achieved with higher sample number.

Out of Band Interference

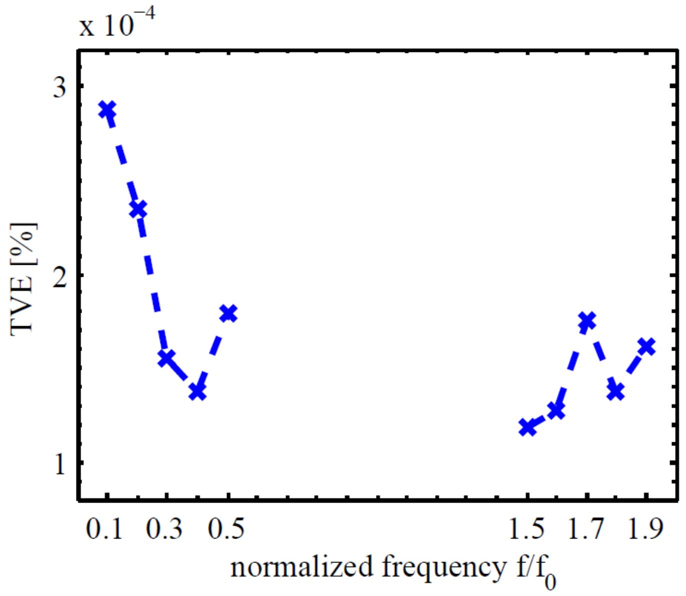

Dependency on ADC Rate

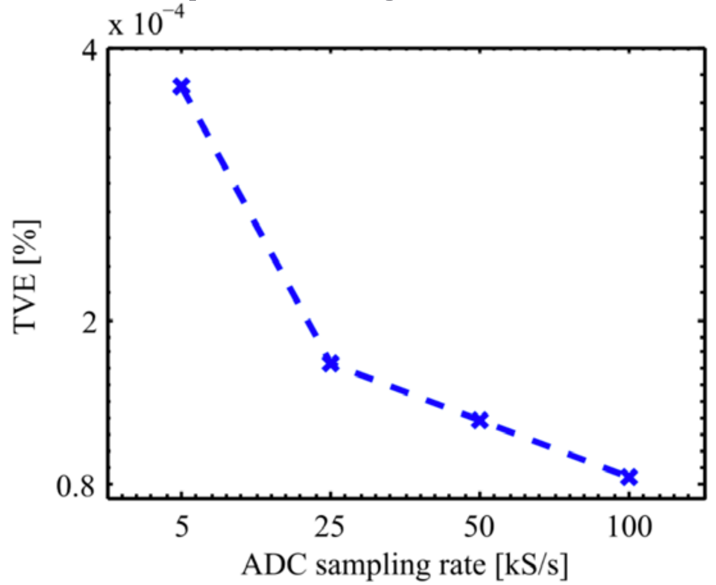

Presentation Outline

- Hardware Architecture
- Metrological Characterization
  - Reference value definition
  - Uncertainty contributions
- Phasor Analysis in Transient Events
- Conclusions

Metrological Characterization

Uncertainty sources

We evaluate the **uncertainty contributions** produced by the different blocks of the **PMU calibrator**, i.e. we perform a thorough **characterization of NI PXI 6682 and 6289 boards**.

We compare the PMU calibrator estimates with the measurement provided by **high-accuracy instrumentation**:

- **Amplitude**: **HP3458A digital voltmeter (DVM)** with a resolution of 1 μV;
- **Frequency**: **SR620 universal time counter (DFM)** with a resolution 10 nHz.
- **Initial Phase**: we consider a 5s waveform processed with **IpDFT [2]** with a resolution of 10 nrad.

NB: hardware instrumentation guarantees optimal performance only in the absence of time variations / interference
➔ error characterization performed only in **steady-state conditions.**

Metrological Characterization

Uncertainty sources

We identify three main error sources:

- **DAC & ADC accuracy** ➔ affects magnitude, frequency and phase uncertainty;
- **Time-base stability** ➔ affects frequency and phase uncertainty;
- **Synchronization** ➔ affects phase uncertainty.

For each source, we consider waveform in steady-state conditions of 5s duration (corresponding to 248 estimates at 50 fps), and characterize the deviation between estimated and measured values in terms of:

1) **mean value**, μ that is fixed ➔ can be **compensated**;

2) **standard deviation**, σ that is random ➔ represents the **actual uncertainty**.

By assuming a **Gaussian error distribution**, in each test we evaluate the **worst-case uncertainty as 3σ range**.

Metrological Characterization

Synchrophasor magnitude uncertainty

In terms of magnitude uncertainty (MU), we compare the NL-LSQ estimates with DVM measurements **(res. ±1 μV)**.
The instrument is triggered by the same clock of DAC / ADC ➔ guaranteed synchronization.

As function of signal frequency, we determine a worst-case uncertainty **MU < 12 μV (1 ppm @ full input range)**

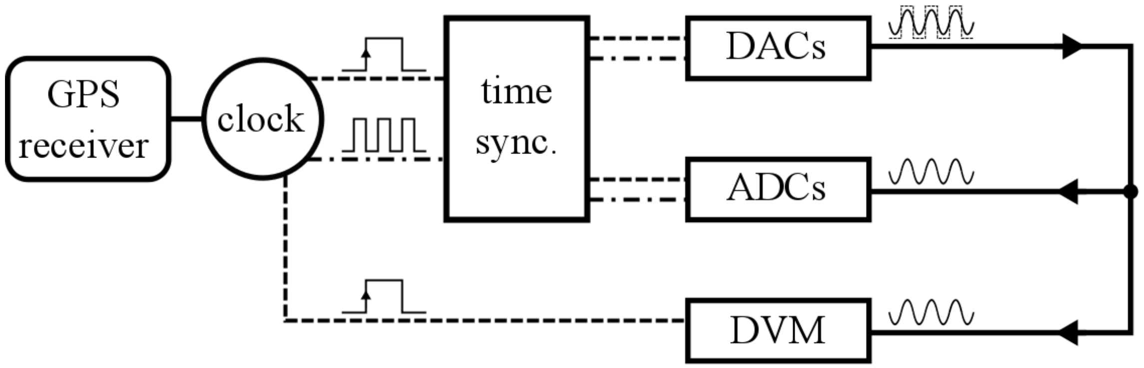

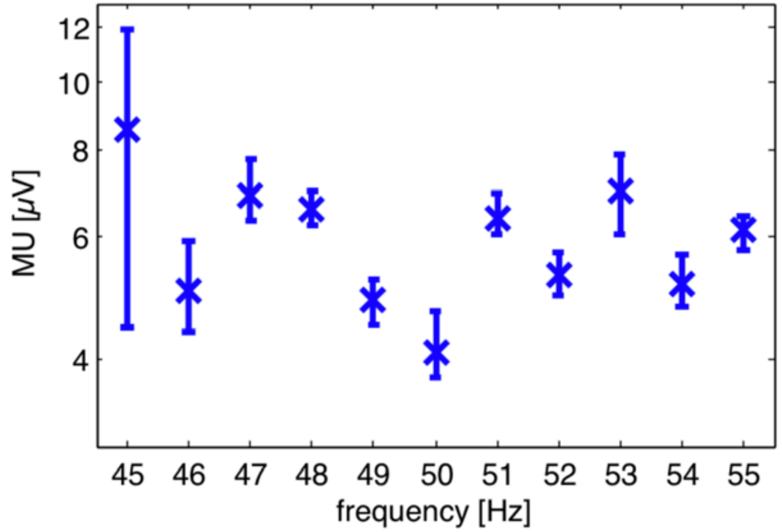

Metrological Characterization

Synchrophasor phase uncertainty

In terms of phase uncertainty (PU), we should consider the contribution due to both frequency and initial phase. To this end, we compare the NL-LSQ estimates with DFM and IpDFT measurements.

The instrument is triggered by the same clock of DAC / ADC ➔ guaranteed synchronization.

As function of signal frequency, we determine a worst-case uncertainty **PU < 0.8 μrad.**

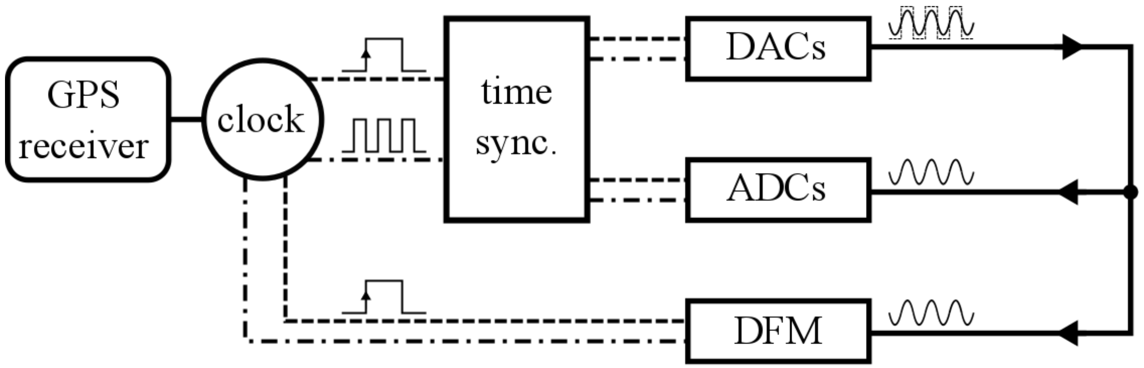

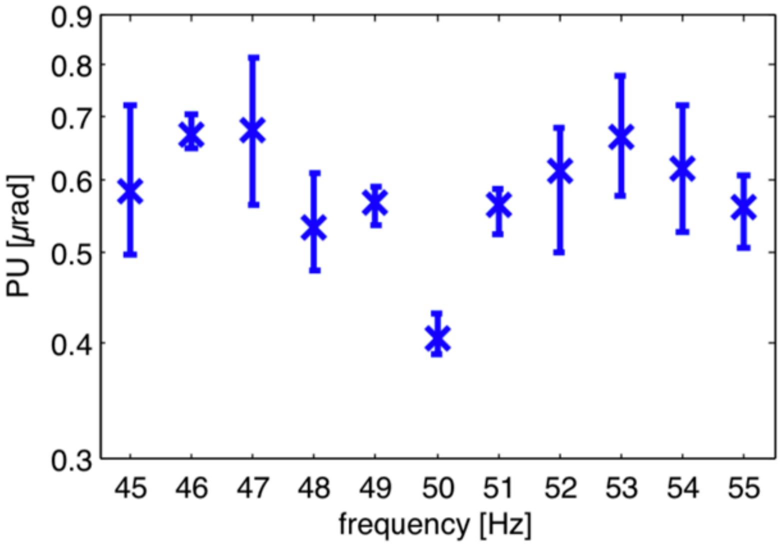

Metrological Characterization

Time reference stability

Time reference error (TE): deviation between PPS of PMU calibrator (PXI-PPS) and UTC-CH (UTC-CH) in METAS.
Over two days, standard deviation ***σ*< 11.5 ns**, that corresponds to a **phase uncertainty of 4 *μ*rad at 50 Hz**.

In METAS, we also compare the **phase noise** obtained in **3 different setups**:

- PXI only;
- PXI + GPS receiver;
- PXI + GPS receiver + atomic clock ➔ **enhanced short-term variability**

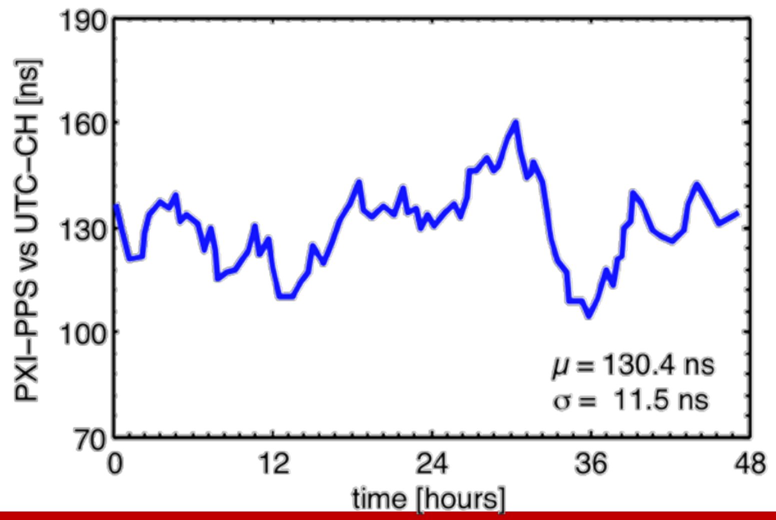

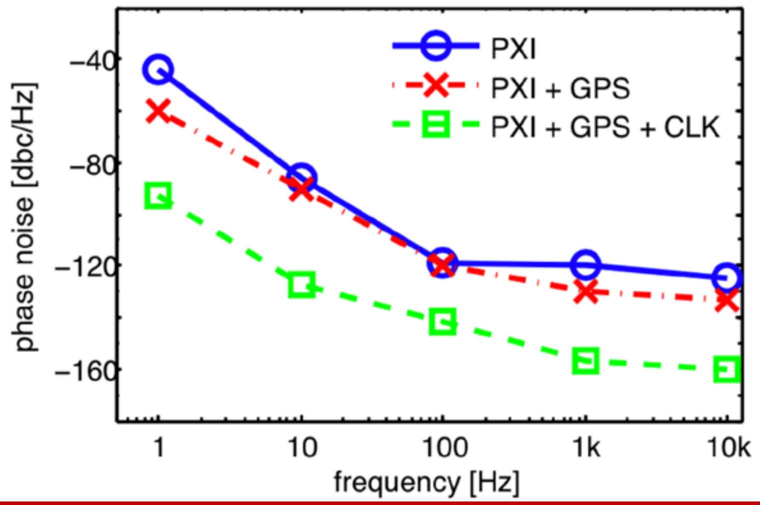

Metrological Characterization

Internal synchronization uncertainty

Synchronization error (SE): initial phase displacement due to **imprecise synchronization between DAC and ADC.**

Three-steps procedure accounts for the initial phase contribution that can vary from experiment to another.

On varying **signal frequency within [10, 1000] Hz**, we obtain a worst case uncertainty **SE < 4.85 μrad**

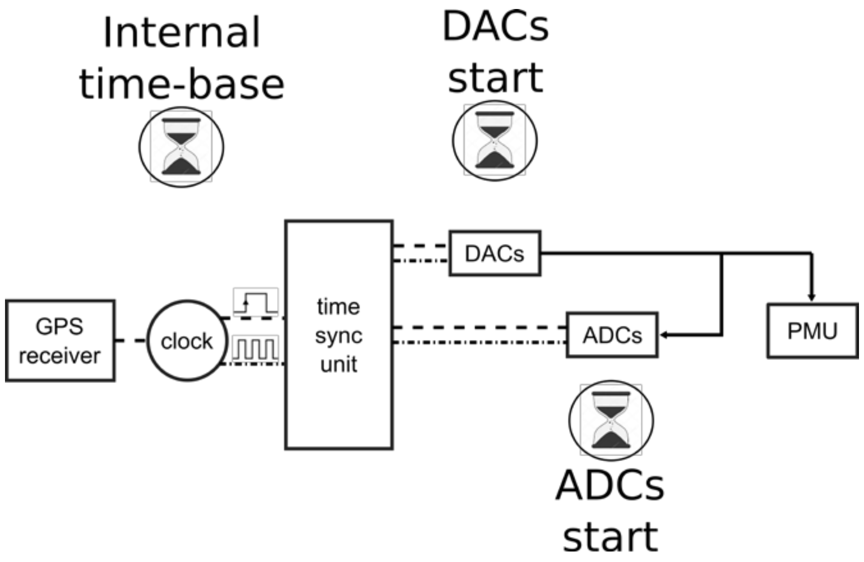

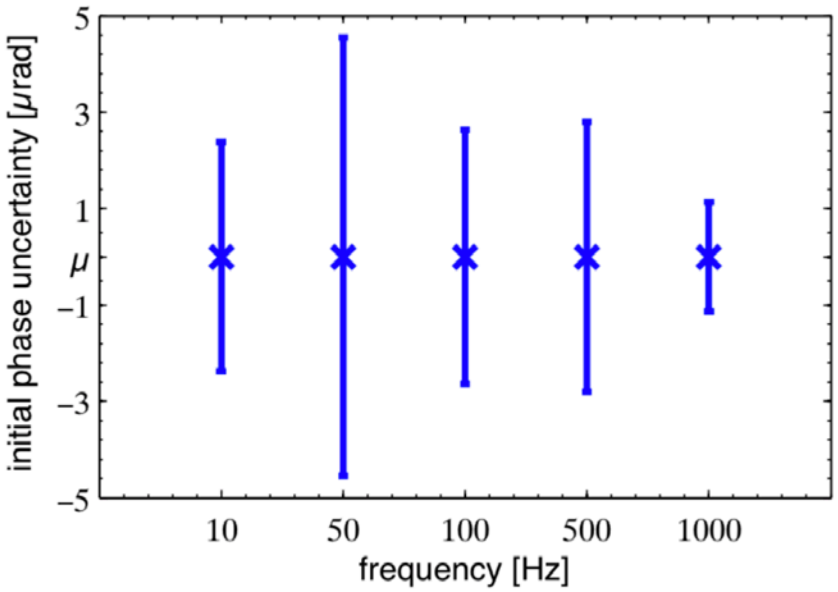

Metrological Characterization

IEEE Std C37.118.1 tests

Based on MU, PU, SE and TE, we characterize the equivalent TVE provided by the PMU calibrator within the entire **test set of IEEE Std C37.118.1**.

Test	TVE [%]	FE [Hz]	RFE [Hz/s]
nominal	$2.03 \cdot 10^{-4}$	$2.29 \cdot 10^{-6}$	$2.29 \cdot 10^{-4}$
signal frequency	$3.56 \cdot 10^{-4}$	$4.31 \cdot 10^{-6}$	$4.31 \cdot 10^{-4}$
harmonic dist.	$1.74 \cdot 10^{-4}$	$4.19 \cdot 10^{-6}$	$4.19 \cdot 10^{-4}$
out-of-band dist.	$4.02 \cdot 10^{-4}$	$1.50 \cdot 10^{-6}$	$1.50 \cdot 10^{-4}$
meas. bandwidth	$3.57 \cdot 10^{-2}$	$1.34 \cdot 10^{-3}$	$1.34 \cdot 10^{-1}$
ampl. modulation	$2.53 \cdot 10^{-5}$	$6.40 \cdot 10^{-5}$	$6.40 \cdot 10^{-3}$
phase modulation	$2.52 \cdot 10^{-2}$	$1.34 \cdot 10^{-3}$	$1.34 \cdot 10^{-1}$
frequency ramp	$9.17 \cdot 10^{-3}$	$4.86 \cdot 10^{-5}$	$4.86 \cdot 10^{-3}$
step change	$4.24 \cdot 10^{-4}$	$7.19 \cdot 10^{-6}$	$7.19 \cdot 10^{-4}$

STEADY-STATE SINGLE TONE
TRUE VALUE← HW INSTRUMENT

STATIC & DYNAMIC TESTS
TRUE VALUE← USER PARAMETERS

Presentation Outline

- Hardware Architecture
- Metrological Characterization
  - Reference value definition
  - Uncertainty contributions
- Phasor Analysis in Transient Events
- Conclusions

Phasor Analysis in Transient Events

Step test implementation

$$x(t) = A\left(1 + A_T \cdot \frac{1}{1 + e^{-k(t-T_T)}}\right) \cdot \cos(2\pi f t + \varphi_0)$$

$\boldsymbol{k}$: determines **the bandwidth** of the transient event

IEEE Std. synchrophasor representation: signal DFT consists of **one / few narrow-band components**, but during step:

- incomplete representation of entire **signal information content**
- PMU accuracy evaluation based on **TVE might loose significance**

Amplitude Envelope

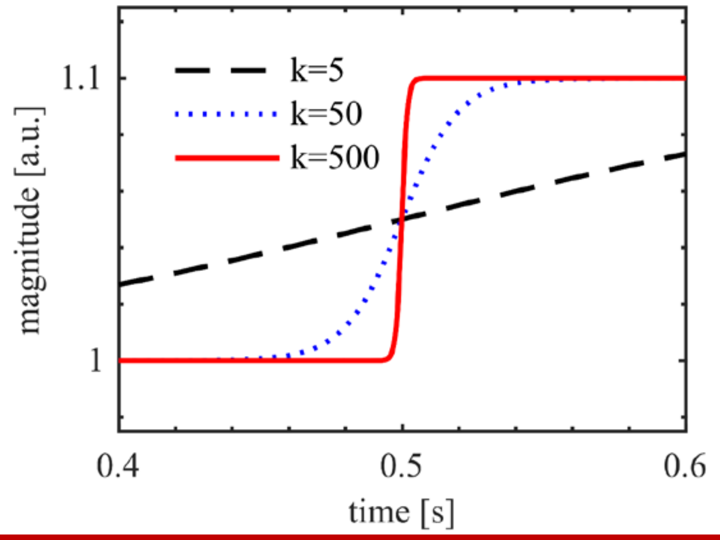

Signal DFT in T_T

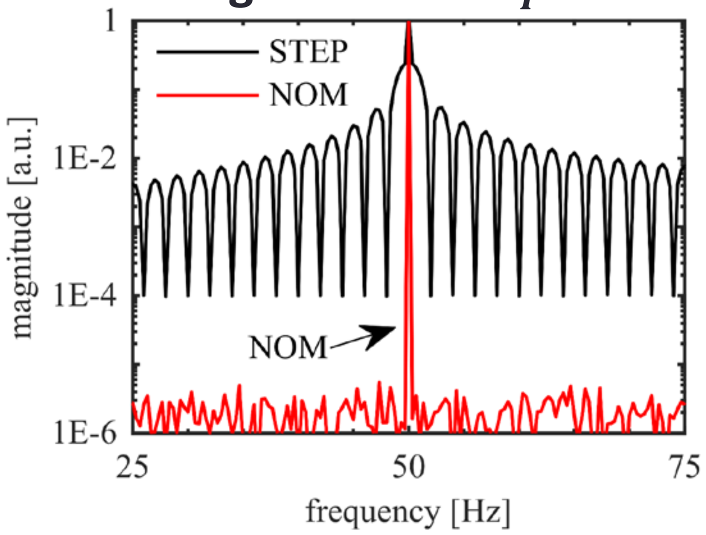

Phasor Analysis in Transient Events

RMSE-based performance evaluation

We compare the performance of three estimation algorithms, **as function of increasing transient bandwidth k**:

- **NL-LSQ** (non-linear fit, **known** signal model) [1];
- **CS-TFM** (**dynamic** signal model) [3];
- **IpDFT** (**static** signal model) [2].

First, we consider the canonical TVE performance evaluation:

- **NL-LSQ**: almost **independent** from k;
- **CS-TFM**: degradation, but **within 1% limit**;
- **IpDFT**: **error diverges** as k increases.

Maximum TVE

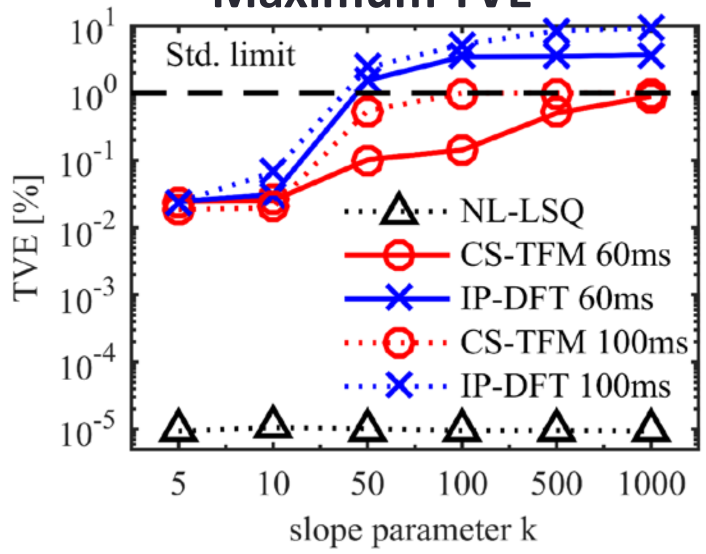

Phasor Analysis in Transient Events

RMSE-based performance evaluation

We compare the performance of three estimation algorithms, **as function of increasing transient bandwidth k**:

- **NL-LSQ** (non-linear fit, **known** signal model) [1];
- **CS-TFM** (**dynamic** signal model) [3];
- **IpDFT** (**static** signal model) [2].

Then, we consider the **RMSE discrepancy** between acquired and recovered fundamental time-domain trend:

$$RMSE = \sqrt{\sum_n \frac{(\hat{x}[n] - x[n])^2}{N_m}}$$

- **NL-LSQ**: performance almost **constant** over time;
- **CS-TFM, IpDFT**: **both error diverge**, in the presence of step.

Time-Domain RMSE

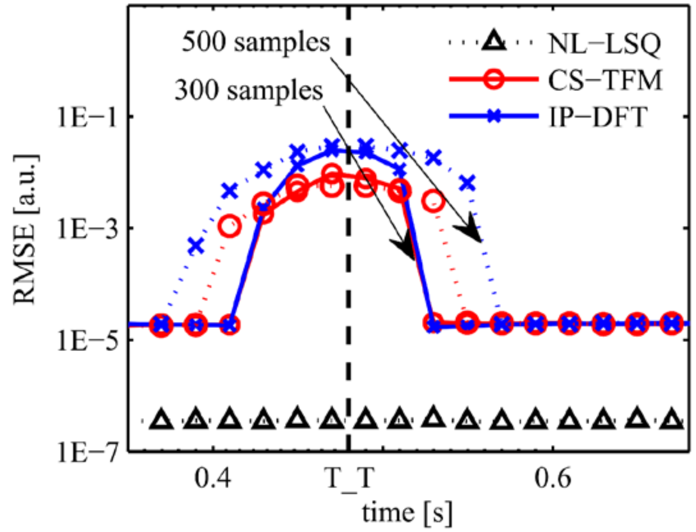

Presentation Outline

- Hardware Architecture
- Metrological Characterization
  - Reference value definition
  - Uncertainty contributions
- Phasor Analysis in Transient Events
- Conclusions

Conclusions

- We have derived the **accuracy requirements** needed by **PMUs operating in ADNs** and discussed the inadequacy of the IEEE Std. C37.118.1, and particularly its 1% TVE limit.

- We have **developed and characterized a highly accurate calibration system** for PMUs in ADNs, that is able to reproduce all the test conditions defined by the IEEE Std. C37.118.1.

- The developed PMU calibrator is characterized by a **TVE ≈ 0.00*x* % in static conditions** and **TVE ≈ 0.0*x* % in dynamic conditions**.

- We have discussed the validity and **appropriateness of TVE as function of the observed signal bandwidth,** and proposed an **alternative performance index** based on the **RMSE** between acquired and recovered fundamental trend **in the time-domain**.

References

[1] G. Frigo, D. Colangelo, A. Derviškadić, M. Pignati, C. Narduzzi, M. Paolone, *"Definition of Accurate Reference Synchrophasors for Static and Dynamic Characterization of PMUs,"* in IEEE Transactions on Instrumentation and Measurement, vol. 66(9), Sept. 2017.

[2] P. Romano, M. Paolone, *"Enhanced Interpolated-DFT for Synchrophasor Estimation in FPGAs: Theory, Implementation, and Validation of a PMU Prototype,"* in IEEE Transactions on Instrumentation and Measurement, vol. 63(12), Dec. 2014.

[3] M. Bertocco, G. Frigo, C. Narduzzi, C. Muscas, P.A. Pegoraro, *" Compressive Sensing of a Taylor-Fourier Multifrequency Model for Synchrophasor Estimation,"* in IEEE Transactions on Instrumentation and Measurement, vol. 64(12), Dec. 2015.

Thank You!

Guglielmo Frigo

Distributed Electrical Systems Laboratory

Email: guglielmo.frigo@epfl.ch
Web: desl-pwrs.epfl.ch

ÉCOLE POLYTECHNIQUE FÉDÉRALE DE LAUSANNE

Motivation of the Work

Two-port equivalent line model

Working HP: a PMU used to monitor an ADN must be capable of correctly measuring the amplitude and phase angle differences at the extremities of a transmission line for both voltage and current phasors.

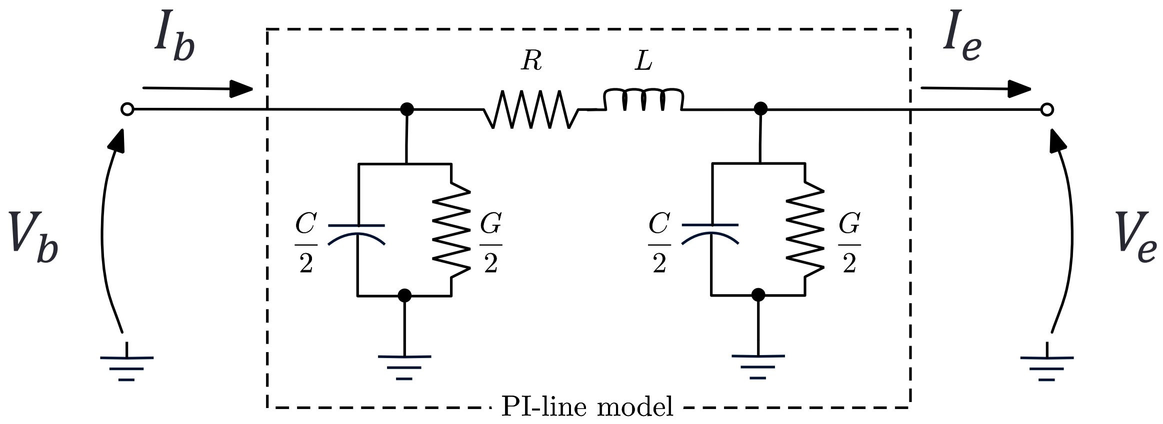

Two-port equivalent model:

$$\begin{bmatrix} V_b \\ I_b \end{bmatrix} = \begin{bmatrix} A & B \\ C & D \end{bmatrix} \begin{bmatrix} V_e \\ I_e \end{bmatrix}$$

Motivation of the Work

Accuracy requirements derivation

1. Definition of scenarios:
   - The nominal voltage of the line $4.16 \leq V_n \leq 36$ [kV]
   - The line type (cable/overhead), and relevant parameters r, c, l, g
   - The line length $100 \leq \lambda \leq 5000$ [m]
   - The line load at the end of the line $(S_e, \cos\varphi_e)$ or, equivalently, (P_e, Q_e)
2. Computation of the the voltage and current phasors at the end of the line:

$$V_e = \frac{V_n + j0}{\sqrt{3}}, \qquad I_e = \left(\frac{P_e + jQ_e}{V_e}\right)^*$$

3. Computation of the voltage and current phasors at the beginning of the line:

$$\begin{bmatrix} V_b \\ I_b \end{bmatrix} = \begin{bmatrix} A & B \\ C & D \end{bmatrix} \begin{bmatrix} V_e \\ I_e \end{bmatrix}$$

4. Computation of the following differences and equivalent TVE:

$$\begin{cases} \varepsilon_{V,m} = |V_b| - |V_e| \\ \varepsilon_{V,p} = \angle V_b - \angle V_e \\ TVE_V = \dfrac{|V_b - V_e|}{V_e} \end{cases}, \quad \begin{cases} \varepsilon_{I,m} = |I_b| - |I_e| \\ \varepsilon_{I,p} = \angle I_b - \angle I_e \\ TVE_I = \dfrac{|I_b - I_e|}{I_e} \end{cases}$$

Motivation of the Work

Simulation Results ➔ Equivalent Voltage TVE

$V_n = 4.16\ kV$

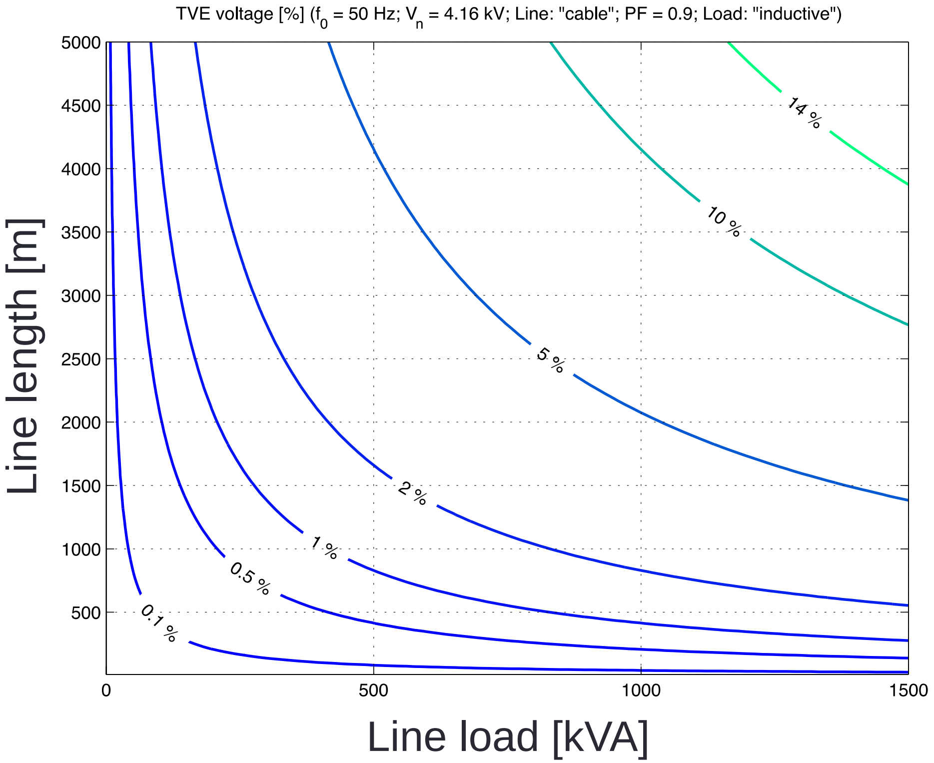

$V_n = 20\ kV$

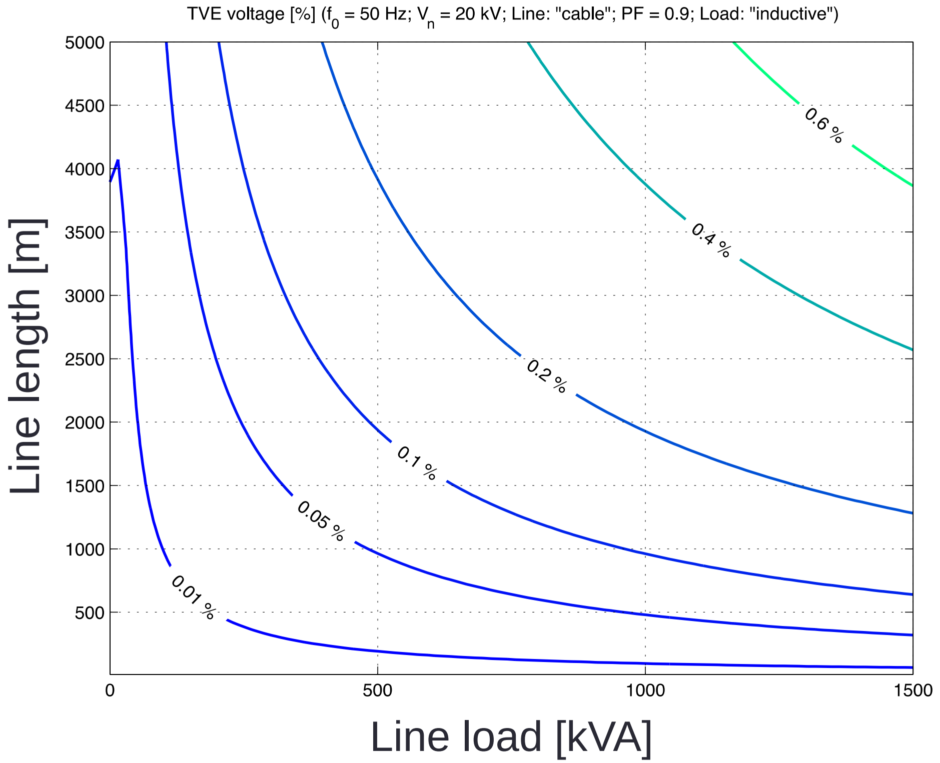

- The equivalent voltage TVE is influenced by both line length and line load and **becomes smaller as the line gets shorter and/or the power flow smaller**
- Particularly with **higher nominal voltages**, the related PMU requirements become quite challenging

Metrological Characterization

NL-LSQ numerical stability

$$\{\hat{A}, \hat{f}, \hat{\phi}_0\} = \text{argmin}_{\hat{\mathcal{P}}} \|x[n] - \hat{x}[n]\|_2$$

The considered optimization problem is **strictly non-convex**, and thus **numerically ill-conditioned**.

The convergence to optimal solution depends on the **initial guess** $\boldsymbol{\mathcal{P}}^* = \{\boldsymbol{A}^*, \boldsymbol{f}^*, \boldsymbol{\varphi}_0^*\}$.

Given the true values $\mathcal{P} = \{1, 50, \pi\}$, the confidence interval that guarantees **convergence to optimal solution $\mathcal{P}^{min}$**

$$A^* = 0.9 \div 1.1 \quad\quad A = 1$$
$$f^* = 48 \div 52 \quad\Rightarrow\quad f = 50$$
$$\varphi_0^* = (\pi \div 3\pi)/2 \quad\quad \varphi_0 = \pi$$

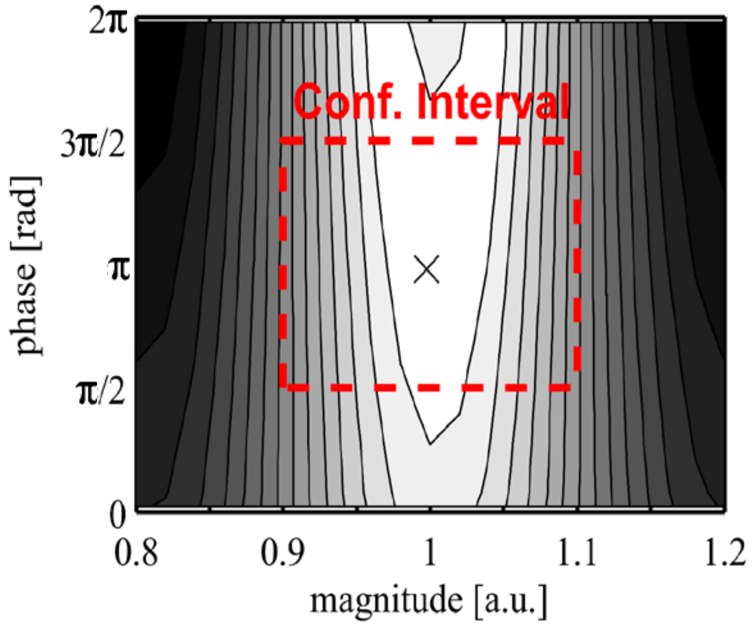

Metrological Characterization

Internal synchronization uncertainty

Synchronization error (SE): initial phase displacement due to imprecise synchronization between DAC and ADC

1) **ADC+DAC initial phase**: typical calibration procedure, signal generated and simultaneously acquired, then processed with IpDFT [2] ➔ $\phi_0^{DAC+ADC}$

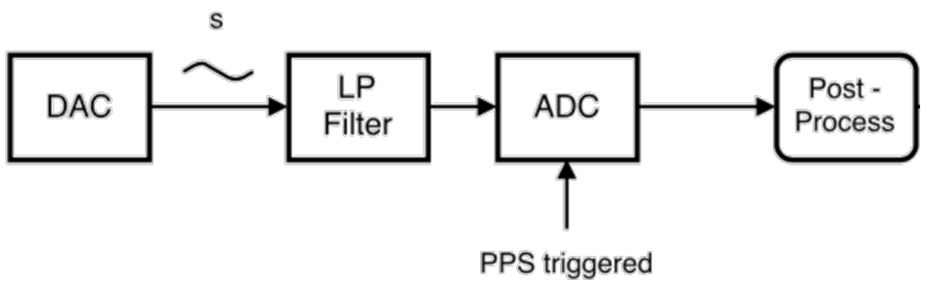

Metrological Characterization

Internal synchronization uncertainty

Synchronization error (SE): initial phase displacement due to imprecise synchronization between DAC and ADC

1) **ADC+DAC initial phase:** typical calibration procedure, signal generated and simultaneously acquired, then processed with IpDFT [2] ➔ $\phi_0^{DAC+ADC}$

2) **ADC initial phase**: subPPS signal derived from internal clock, synchronously acquired by ADC and processed with IpDFT [1] ➔ ϕ_0^{ADC}

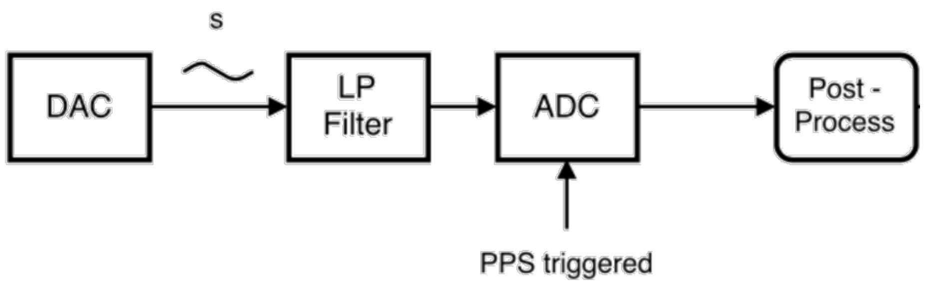

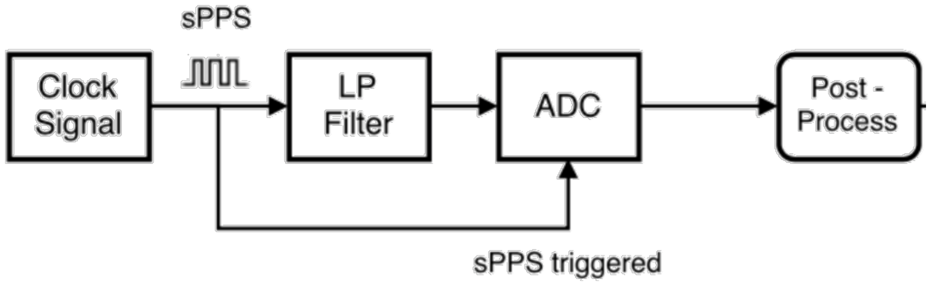

Metrological Characterization

Internal synchronization uncertainty

Synchronization error (SE): initial phase displacement due to imprecise synchronization between DAC and ADC

1) **ADC+DAC initial phase:** typical calibration procedure, signal generated and simultaneously acquired, and processed with IpDFT [2] ➔ $\phi_0^{DAC+ADC}$

2) **ADC initial phase**: subPPS signal derived from internal clock, synchronously acquired by ADC and processed with IpDFT [2] ➔ ϕ_0^{ADC}

3) **"Only DAC" initial phase:** subtraction of 1) – 2) ➔ $\phi_0^{DAC+ADC} - \phi_0^{ADC} = \phi_0^{DAC}$

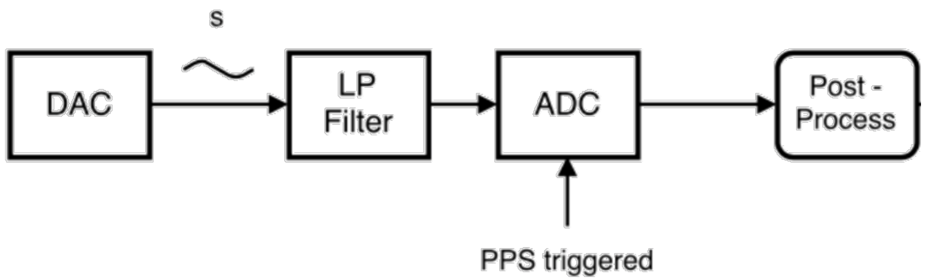

[redacted]

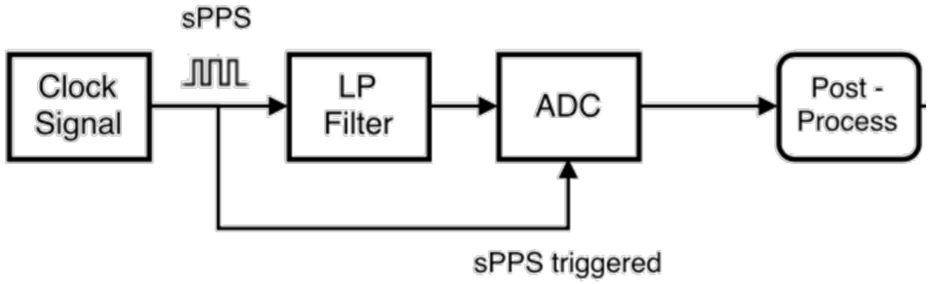

Metrological Characterization

Phase definition in transient

Actual metering devices sense steps (particularly phase/frequency) not only as a succession of two different steady-state conditions, but as large frequency (and thus ROCOF) variations

➔ problems for frequency-based applications (e.g. load shedding)

Possible solutions:

1) Enlarging the window length ➔ worse response time;

2) More complex signal models to account for time-varying trend ➔ increased complexity

   – Static signal model (Fourier series analysis) $x(t) = A(t) \cdot \cos(2\pi f t + \phi_0) = A(t) \cdot \cos\big(\theta(t)\big)$

   – Taylor-Fourier signal model (Frigo et al.) $x(t) = \Re\left\{\sum_k \frac{t^k}{k!}\left[\frac{p^k}{\sqrt{2}}\, e^{1j2\pi f t} + \frac{(p^k)''}{\sqrt{2}}\, e^{-1j2\pi f t}\right]\right\}$

   – Underlying freq. signal model (Kirkham et al.) $x(t) = A(t) \cdot \cos\big(\theta(t) + \psi(t)\big)$

Metrological Characterization

Performance indices

Given a general sinusoidal signal and the corresponding synchrophasor representation

$$x(t) = A(t) \cdot \cos\big(2\pi f(t)t + \phi_0(t)\big) = A(t) \cdot \cos\big(\psi(t)\big) \qquad X(t) = A(t) \cdot e^{1j\,\psi(t)}$$

and the estimated quantities $\hat{A}$, $\hat{f}$, $\widehat{\phi_0}$, we can retrieve the time-domain and synchrophasor representations:

$$\hat{x}(t) = \hat{A}(t) \cdot \cos\left(2\pi \hat{f}(t)t + \widehat{\phi_0}(t)\right) \qquad \hat{X}(t) = \hat{A}(t) \cdot e^{1j\,\hat{\psi}(t)}$$

Performance indices to assess the estimation accuracy:

1) TVE (IEEE Std) relies on synchrophasor model

2) RMSE (Frigo et al.) relies on time-domain

$$RMSE = \sqrt{\sum_n \frac{(\hat{x}[n]-x[n])^2}{N_m}}$$

3) GoF (Kirkham et al.) accounts also for model d.o.f.

$$GoF = 20 \log \frac{A}{\sqrt{\frac{1}{(N-m)}} \cdot \sqrt{\sum_n (x[n]-\hat{x}[n])^2}}$$